ICCK Transactions on Electric Power Networks and Systems
http://dx.doi.org/10.62762/TEPNS.2025.127082

RESEARCH ARTICLE

Check for updates

Simulation of Thermal Operation Modes of XLPE Pulse Cable

Evgenii Chesnokov[1], **Efrem Feklistov**[2], **George Greshnyakov**[2] **and Oleg Emelyanov**[2,*]

[1] Higher School of High Voltage Engineering, Peter the Great St.Petersburg Polytechnic University (SPbPU), 195251, St.Petersburg, Russia

Abstract

The results of numerical simulation of temperature modes of cross-linked polyethylene (XLPE) cable under transient states for International Thermonuclear Experimental Reactor (ITER) application are presented. The pulsed electric current load in the external circuit rapidly changes with the maximum values of 1.5 kA during tens of seconds decay with a period of 1200 s that corresponds to operation modes of the ITER fusion reactor. The core temperature achieves periodic steady-state at 20000 s, which is consistent with 4-5 cable thermal constant (4500 s). The numerical results obtained reveal that the skin effect plays an insignificant role on core temperature dynamics. Multiphysics model links electric current with heat generation in cables with respect to electromagnetic effects and measured temperature dependencies of electro and thermophysical properties of the cable's XLPE insulation.

Keywords: pulse cable, skin effect, temperature transient state, thermophysical property of cross-linked polyethylene (XLPE).

Submitted: 04 August 2025
Accepted: 14 September 2025
Published: 19 October 2025

Vol. 1, **No.** 1, 2025.
10.62762/TEPNS.2025.127082

***Corresponding author:**
Oleg Emelyanov
oaemel2@gmail.com

1 Introduction

International Thermonuclear Experimental Reactor (ITER) is a nuclear fusion facility, where it demands extensive integration of many cable systems interfaces with varying functional and physical characteristics. The cable requirement data form a giant cable database with scope for approximately 120,000 cables in total, with cables spanning more than 12,000 km to be installed within approximately 200 km of cable trays [1, 2]. Some cables with high current capacity are used in power devices, special-purpose ones operating in pulsed modes. The problems that arise in the design and manufacture of special low-inductance impulse cables (SLIC) for power supply and protection of the superconducting magnetic system of the ITER reactor were presented in [3]. It is known that the capacity of medium and high voltage cables strongly depends on the temperature regime, which is affected by many factor, and it is necessary to predict changes in cable temperature. Nevertheless, the known early classical analytical solutions of temperature dynamics can be used only for simple cylindrical geometries and loads. In cases of complex cable structures, pulsed loads, taking into account the temperature dependences of electrical and thermal properties of materials, no exact solutions are known.

To assess the thermal state of a cable, the thermoelectric equivalent method (TEE) has found wide application, which essentially uses the approximation of a regular

Citation
Chesnokov, E., Feklistov, E., Greshnyakov, G., & Emelyanov, O. (2025). Simulation of Thermal Operation Modes of XLPE Pulse Cable. *ICCK Transactions on Electric Power Networks and Systems*, 1(1), 17–25.

thermal regime. At the design stage, the transmission capacity of the cable is determined using the TEE method described in IEC 60287, which proposes taking into account a large number of correction factors. The calculation the temperature of cables laid in channels, pipes, etc. can be done by using the empirical formulas [4] and IEC 60287, IEC 60853 and SIGRE standards [5–9]. The IEC 60287 describes the methods of temperature calculation, taking into account the cable design, skin effect, proximity effect and temperature coefficient of resistance, screen grounding method, cable arrangement, environmental conditions, etc. The methods from the IEC 60853 standard allow calculating the dynamics of cable temperature only for a constant load over time. It is obvious that the maximum temperature will occur in those insulation layers that are directly adjacent to the core. Therefore, when calculating the long-term permissible load current, the condition of not exceeding the core temperature must be met (for example, for short terms conditions of cross-linked polyethylene (XLPE) $T_c \leq 130°\text{C}$).

At the same time, the number of Finite Element Method (FEM) software packages (ANSYS, COMSOL Multiphysics, ELCUT, etc.) are used for thermal and electromagnetic fields calculations [10–14]. The advantage of using these programs in comparison with the IEC 60287 methodology is that they allow one to take into account any cable line design, solve nonlinear problems, build multiphysics models that link electric current with heat generation in cables taking into account electromagnetic effects (for example, joint calculation of thermal and electromagnetic fields.

The combination of finite element method and thermoelectric equivalent method for cable dynamic thermal rating presented in [12], where was shown that using IEC recommended transient thermal model of cable insulation will bring certain error to cable dynamic temperature evaluation, especially at the early stage of cable temperature rise. Thermal Analysis of Cables under Harmonic Load Currents was performed by lumped model TEE according to IEC 60853-2 and Comsol software [13]. In addition, the simulations of cable parameters were successfully carried out using COMSOL Multiphysics software based on the FEM [14]. The models described in [10–14] are the most universal and allow taking into account the largest number of factors affecting the transmission capacity of the cable line. In addition, they allow calculating temperature dynamics, but in this case, high processor performance and a large amount of computer Random Access Memory (RAM) are required to reduce the calculation time. At the same time, most of the works (see the latest CIGRE brochure [5] and numerous references therein) are devoted, as a rule, to the calculation of steady-state modes in underground or submarine cables at industrial frequency, and the pulse processes are almost never considered in the literature. Some operating modes of cables for ITER have a single or rarely periodic pulse nature (the repetition period exceeds 20 min), in which the pulse duration is several tens of seconds, and the duty cycle reaches values of 60 or more. The article considers exactly such modes, while the originality of the contribution lies in the creation of a coupled electromagnetic model. This allows improving the methodology for calculating pulse cables operating under high-amplitude currents conditions and low duty cycles, taking into account the skin effect and the nonlinear temperature dependence of the XLPE thermophysical parameters.

The article continues the previously completed studies of calculations for pulsed mode of cable operation for the ITER fusion reactor [15, 16], and contains an analysis of the skin effect and the temperature thermal properties of the insulation influences on the cable thermal state.

2 The cable design

Three types of cables are used in the ITER block for switching processes. All of them have the same design and differ only in the cross-section of the conductors (25,120,300 mm^2). The article considers the cable with 25 mm^2 copper core section and insulation made of silane-crosslinked polyethylene. The cable's geometric parameters are shown in Table 1. Figure 1 shows the cable design.

Table 1. The main parameters of designed cable.

Structural layer	Thickness (mm)	Outer diameter (mm)
Inner copper conductor S = 25 mm^2	-	6.3
XLPE inner insulation layer	5.7	18.9
External copper conductor S = 25 mm^2	1.1	22.8
XLPE external insulation layer	5.7	36.2
Copper sheath	0.1	37.8
HDPE outer jacket	1	40

The principle of operation of a pulse cable and the purpose of each individual element of its construction is explained in [3].

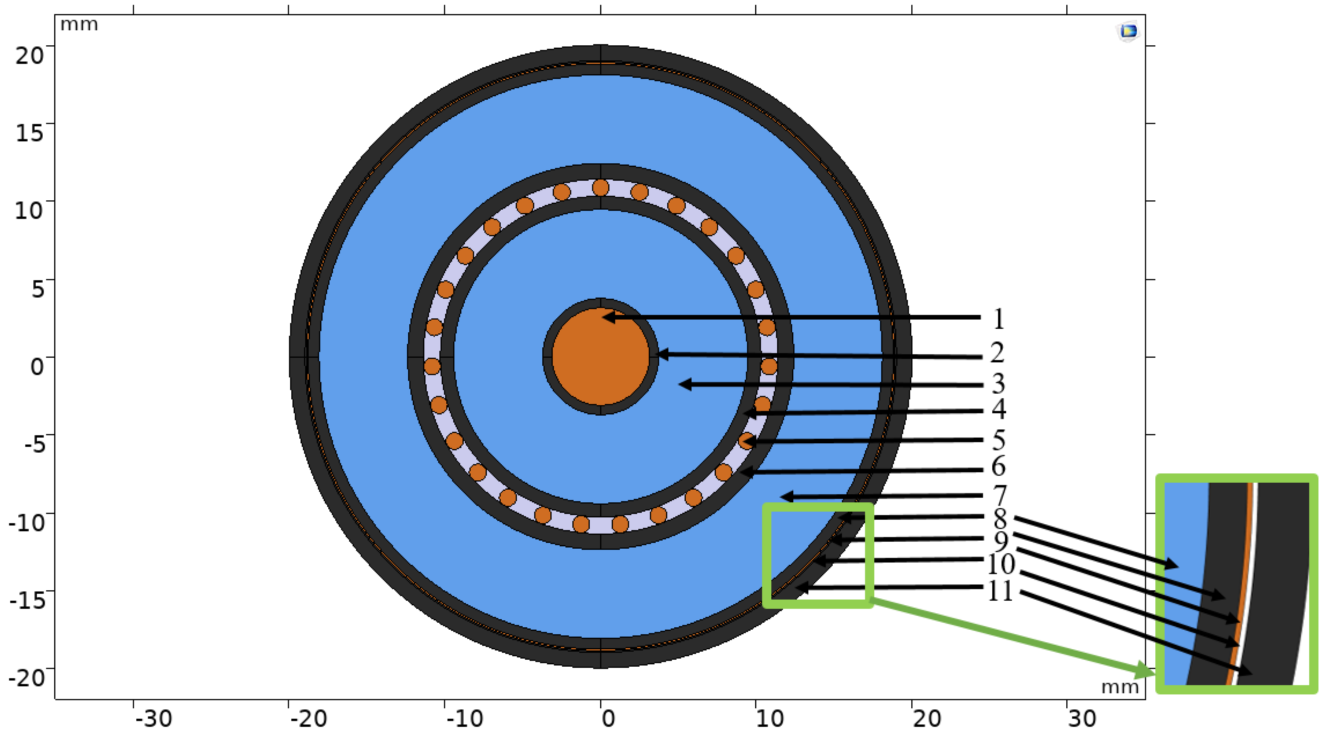

Figure 1. Schematic design of the pulse cable. Representation of pulsed cable; 1 – inner copper conductor, 2 – semi-conducting screen on an inner conductor, 3 – inner XLPE insulation layer, 4 – semi-conducting screen on an insulation layer, 5 – external copper conductor, 6 – semi-conducting screen on an external conductor, 7 – external XLPE insulation layer, 8 – semi-conducting screen on an insulation layer, 9 – copper sheath, 10 – polyethyleneterephthalate (PET) tape, 11 – high density polyethylene (HDPE) outer jacket.

3 The operation modes of ITER cable

The cable is designed for sequential current pulses with a rise time of $t = 10\,\text{ms}$, an exponential decay with a time constant of $\tau = 5 - 20\,\text{s}$. The current amplitude is $I = 1.5\,\text{kA}$, and the pause between the pulses should be at least 20 minutes. The service life of a cable should be at least 30,000 pulses. For the calculations given below, the worst calculation conditions were set, namely, the pulse time constant $\tau = 20\,\text{s}$ and a pause between pulses of 20 minutes. Compared to a single pulse mode, the steady-state periodic pulse mode (the repetition period 20 min) corresponds to the most stressful condition that was regulated by special ITER requirements. The current pulse shape and scaling view are shown in Figure 2.

Figure 2 shows the calculated graph of a current pulse with a maximum value of $\tau = 20$ s. For better understanding, the callout to the graph shows the front of a current pulse, which has a characteristic time scale duration of ~ 10 ms. Also, despite the fact that the graph on the X-axis shows the time up to 200 s, it is worth remembering that the pause between pulses is 1200 s (20 minutes) and this time scale was given for a better understanding of the current pulse shapes.

4 The governing equations for computation model

Electromagnetic–Thermal simulation was based on Comsol Coupling Model that takes into account the electromagnetic and heat transfer characteristics, including appropriate boundary conditions and temperature dependencies of the heat transfer coefficients as follows:

1. The main parameters of the electromagnetic field (Maxwell equations):

$$\begin{aligned} \nabla \times \vec{H} &= \vec{J_c} + \frac{\partial \vec{D}}{\partial t}, \\ \nabla \times \vec{E} &= -\frac{\partial \vec{B}}{\partial t}, \\ \vec{B} &= \nabla \times \vec{A}, \\ \nabla \cdot \vec{B} &= 0, \\ \nabla \cdot \vec{D} &= \rho_q, \end{aligned} \tag{1}$$

where H in A/m is the magnetic field intensity,

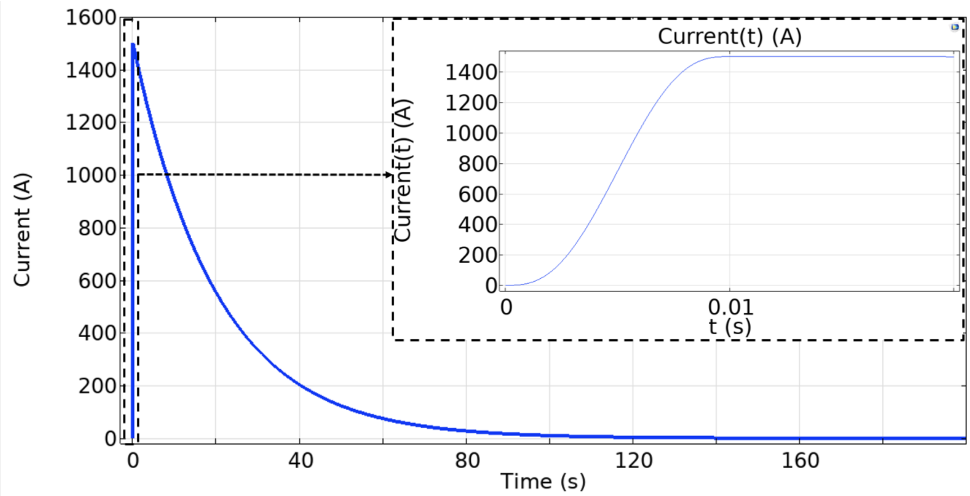

Figure 2. The current pulse shapes.

J in $\mathrm{A/m^2}$ is the current density, D in $\mathrm{C/m^2}$ is the electric displacement, E in V/m is the electric field intensity, B in T is the magnetic induction intensity, A in $\mathrm{T \cdot m}$ is magnetic vector potential, and ρ_q in $\mathrm{C/m^3}$ is the charge density. The definition of the boundary condition of magnetic insulation on the outer surface of the cable was $\vec{n} \times \vec{A} = 0$, where $\vec{n}$ is the normal vector to the outer surface.

2. The relationship among the relevant field vectors is represented by the following material relations

$$\begin{aligned} \vec{B} &= \mu_r \mu_0 \vec{H}, \\ \vec{D} &= \varepsilon_r \varepsilon_0 \vec{E}, \\ \vec{J_c} &= \sigma \vec{E}, \end{aligned} \quad (2)$$

where ε_r is the dielectric constant, μ_r is the permeability, and σ in S/m is the conductivity.

3. The heat transfer equation (3) was used for temperature field calculations:

$$\frac{\partial(\rho C_p(T) T)}{\partial t} + \operatorname{div}(\lambda(T) \operatorname{grad}(T)) + q_v = 0, \quad (3)$$

where ρ is the mass density ($\mathrm{kg/m^3}$), $C_p(T)$ is the specific heat ($\mathrm{J/(kg \cdot K)}$), T is the absolute temperature (K), $\lambda(T)$ is the thermal conductivity ($\mathrm{W/(m \cdot K)}$), and q_v is the volume power of heat sources in inner and external copper conductors in $\mathrm{W/m^3}$:

$$q_v = j^2 \rho_{\mathrm{cu}}, \quad (4)$$

where j — current density (skin effect must be taken into account) ($\mathrm{A/m^2}$), and ρ_{cu} — copper resistivity ($\Omega \cdot \mathrm{m}$).

4. Because of XLPE thermo-physical data are not available in the COMSOL material library, the characteristics of thermal conductivity and heat capacity were obtained on samples of silane-crosslinked polyethylene that are shown in Figure 3. The data in Figure 3 were presented in [3], where thermophysical parameters were obtained using the IT-lambda-400 and IT-C-400 devices with an error no greater than 5% in the temperature range of 0-160 °C.

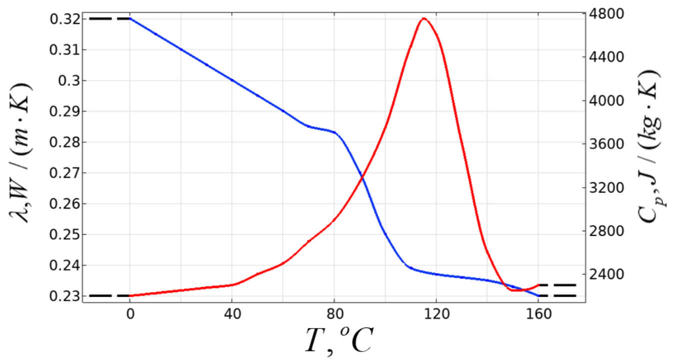

Figure 3. Variation of the thermal conductivity and specific heat of the XLPE insulation with temperature.

The actual characteristics of the insulation were used in the numerical calculation. The measurements were carried out because of quite different XLPE thermal-physics data presented in literature [17–19].

5. At the external cylindrical cable surface, a convective boundary condition can be applied,

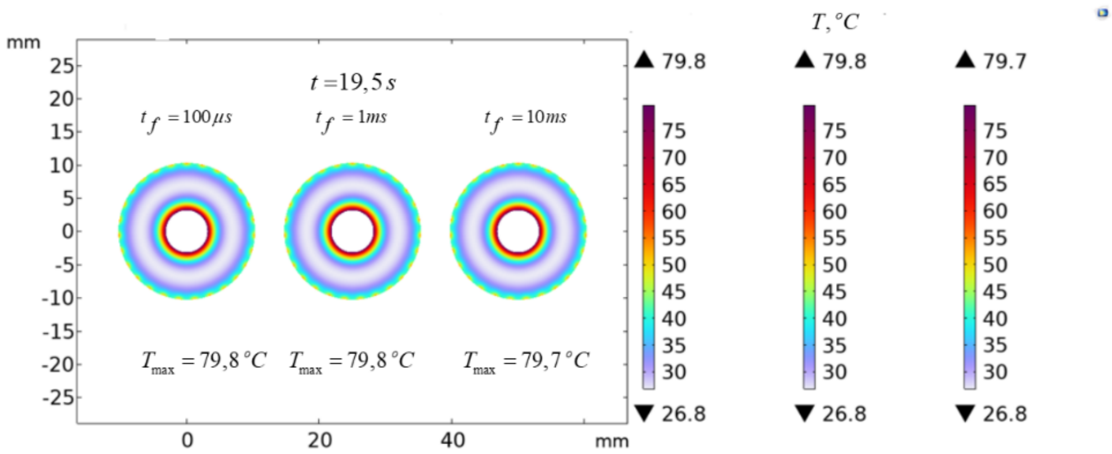

Figure 4. Skin effect influence on conductor temperatures.

which is expressed as:

$$q = h(T_s - T_{\text{amb}}) = -\lambda(T)\left(\frac{\partial T}{\partial n}\right)_S, \qquad (5)$$

where λ is the thermal conductivity of the jacket, h is the heat transfer coefficient due to convection between the cable surface and the surrounding air, which is set as 7 W/(m^2· K); T_S is the temperature at the jacket; and T_{amb} is the temperature of the air, which is presumed as 25°C and it was used as an initial temperature. The definition of the boundary condition of convection on the outer surface of the cable with a convection coefficient of 7 W/(m^2· K) was provided by the design recommendations of the ITER researchers. This characteristic value corresponds to horizontal cable laying in air. If necessary, other types of boundary conditions can be easily taken into account in the COMSOL software ver. 6.2 if this has practical significance.

5 Results and discussion

In the results of the calculation, temperature dynamics values on the surface of the inner conductor were obtained. As mentioned earlier, the calculations took into account the skin effect influence on the temperature of the conductors (inner and external copper conductors). The main impact on the skin effect is due to current pulse front. The results obtained showed that the rise time of the current does not affect the temperature of the conductor (Figure 4). Figure 4 shows that for the different pulse fronts (100 μs–10 ms) the maximum temperature of the inner conductor after the first current pulse does not exceed 80 °C at $t = 19.5$ s, and the temperature difference does not exceed 0.1 °C for the specified current pulse fronts. Additional calculations show that the pulse duration, which depends on τ_t, has the greatest effect on temperature values. For a more accurate solution of the electrothermal problem, the model used a grid with user settings that made it possible to set a smaller step in areas with large temperature gradients.

The model used a refined grid near the surface of the conductors to account for the skin effect. For example then $t_f = 100$ μs. The characteristic size of the finite element (FE) within the skin depth $\delta = 0.67$ mm of the order of $\Delta_1 = \delta/6 = 0.01$ mm. This size ensured good convergence of the grid to the desired solution. With an increase in the FE size, a divergence of the solution was observed, which disappeared when choosing a FE of less than 0.01 mm.

It is worth noting that the use of temperature dependences of material properties significantly increases the time required to calculate the model. Therefore, a numerical simulation was conducted in which two calculation methods were compared: using the temperature dependences $\lambda(T)$ and $C_p(T)$ (see the blue curve in Figure 5), as well as for constant values obtained as the average values from the graph $\lambda_{\text{av}} = 0.272$ W/(m·K) and $C_{p,\text{av}} = 2964$ J/(kg·K) in Figure 3 that corresponds to green curve in Figure 5. The average values can be applied in the further calculations. It is worth noting that the average values of thermal conductivity and heat capacity are quite close to the literature data from [20]: $\lambda = 0.286$ W/(m·K) and $C_p = 3043$ J/(kg·K).

The results obtained showed that the use of averaged values in the calculation of a single pulse and periodic pulses makes it possible to calculate the temperature with sufficient accuracy.

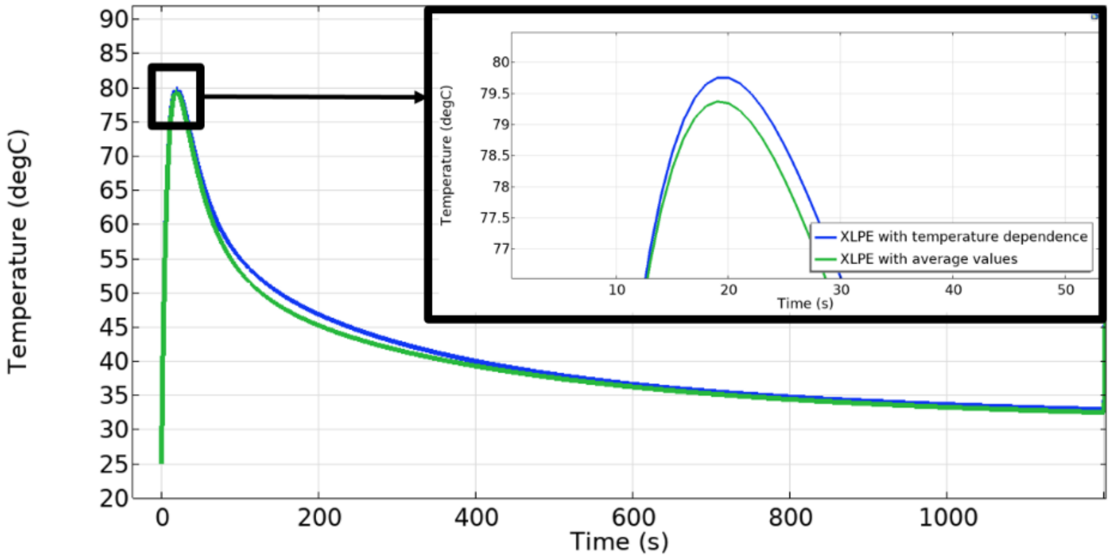

Figure 5. Temperature pulses of the inner conductor.

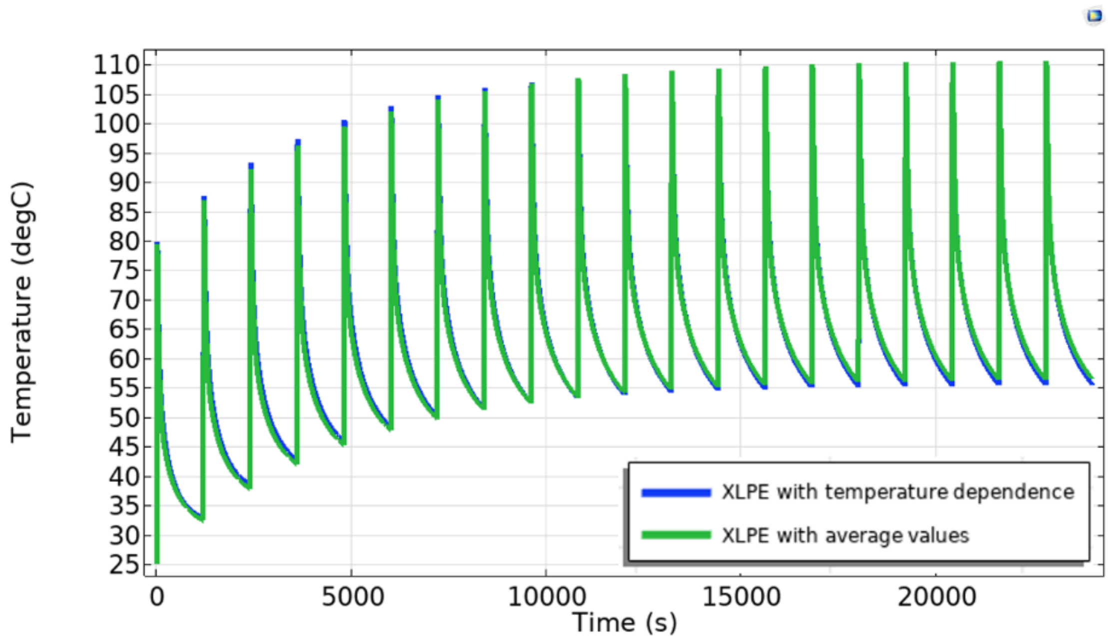

Figure 6. Temperature steady-state mode during application of 20 current pulses.

Figure 6 illustrates the periodic steady-state temperature profile achieved after 20 current pulses, confirming the convergence to thermal equilibrium within approximately 20,000 s. The following modules were used in calculations: Magnetic fields, Heat transfer in solids and Electromagnetic heating in Multiphysics. Two main functions were calculated: the scalar temperature field, T, and the vector magnetic potential, A, with three scalar components (A_x, A_y and A_z), respectively. The desired fields were considered parallel-plane, that is why the problem was solved in a two-dimensional formulation.

The computed domain was discretized using Quadratic Lagrange finite elements, and the largest element size did not exceed 10% of the characteristic thickness of each element of the pulse cable. The model used a refined grid near the surface of the conductors to account for the skin effect. For example, for the current pulse with $t_f = 100$ μs, the characteristic size Δ_1 of the finite element (FE) within the skin depth $\delta \sim 0.67$ mm of the order of $\Delta_1 = \delta/6 = 0.1$ mm. This size ensured good convergence of the grid to the desired solution. With an increase in the FE size, a divergence of the solution was observed, which disappeared when choosing a FE size less than 0.16 mm. Solver type - time dependent, time step set as 0.5 s. The time-stepping method for the problem was backward differentiation formula (BDF). BDF maximum order set as 5, minimum set as 1. To automate the selection of time steps, the Events interface also was used. Convergence criteria for calculated fields were error indicators for the time-dependent solver as follows. The used error indicator is the L_2 norm of the dependent field gradient (e.g. for the temperature in a 2D heat transfer model sqrt(comp1.Tx^2+comp1.Ty^2)). As well known, the gradient of the dependent field is the default value for the error indicator in most physics interfaces in COMSOL Multiphysics. A solution on the finite element mesh is computed in the next time interval after previous one, and the error indicator is evaluated to control the convergence of the problem. Numerical simulation took place on the workstation "ATX-SYS S2066RUO", 32 Gb RAM, with COMSOL 6.2.

The numerical calculation time of one pulse was about 8 hours, and the calculation of 20 pulses with access to steady-state mode took around 95 hours of Comsol calculation. In this case, high processor performance and a large amount of computer RAM are required to reduce the calculation time.

6 Conclusion

(1) The results of numerical modeling of electrical and temperature characteristics of XLPE cable in steady-state and transient modes for use in ITER are presented. The pulse current load in the external circuit changes rapidly with maximum values of 1.5 kA for tens of seconds with a period of 1200 s, which corresponds to the operating modes of the ITER reactor. The inner conductor temperature reaches a periodic steady state in 20,000 s, which corresponds to a cable thermal constant of 4-5 (4500 s).

(2) The maximum value of cable insulation temperature obtained is around of 110 °C. For cross-linked polyethylene, the maximum permissible temperature in overload mode is 130 °C. The cable can be at this temperature for no more than 1000 hours during its entire service life. The service life is determined by the number of pulses equal to 30,000 according to ITER requirements. Therefore, with a high degree of the probability the cable maintains its insulating properties in such operating modes.

(3) The numerical results obtained show that the skin effect plays an insignificant role in the conductors temperature dynamics. This result is easily explained by the relatively long duration of the current pulse. For the different pulse fronts (100 μs–10 ms) the maximum temperature internal conductor after the first current pulse does not exceed 80 °C at $t = 19.5$ s and the temperature difference for the specified range of pulse fronts does not exceed 0.1 °C.

(4) The numerical simulations were conducted using the temperature dependencies $\lambda(T)$ and $C_p(T)$ for XLPE, as well as for their constant average values $\lambda_{\text{av}} = 0.272$ W/(m·K) and $C_{p,\text{av}} = 2964$ J/(kg·K). The results obtained showed that the use of averaged values in the calculation of a single pulse and periodic pulses makes it possible to calculate the temperature with sufficient accuracy. The average values can be used in further calculations because of the using the averaged parameters significantly reduces the calculation time for the task.

(5) The novelty and the originality of the work based on the improving methodology for calculating of pulse cables operating under high-amplitude currents conditions and low duty cycles, taking into account the skin effect and the nonlinear temperature dependence of the thermophysical parameters of cable structural elements on the temperature.

Specific areas of further research will be aimed to improving the calculation model based on mathematical methods in order to significantly reduce the calculation time, taking into account other cables designs, including various cooling conditions (underground installation, solar radiation, etc.)

Data Availability Statement

Data will be made available on request.

Funding

This work was supported without any funding.

Conflicts of Interest

The authors declare no conflicts of interest.

Ethical Approval and Consent to Participate

Not applicable.

References

[1] Sonara, J., Beltran, D., Pintea, B., Hourtoule, J., Benfatto, I., Kim, S. H., ... & Lee, C. J. (2015). An overview of the ITER cabling network and cable database management. Fusion Engineering and Design, 96, 957-960. [CrossRef]

[2] Gung, C. Y., Ilin, Y., Dolgetta, N., Chen, Y., Bauer, P., Jong, C., ..., & Ding, K. (2012). Progress in design, analysis, and manufacturing studies of the ITER feeders. *IEEE Transactions on Applied Superconductivity, 22*(3), 4800804-4800804. [CrossRef]

[3] Doronin, M., Greshnyakov, G., & Korovkin, N. (2018). Modes of operation and design features of pulse cables for the ITER project. In *MATEC Web of Conferences* (Vol. 245, p. 13001). EDP Sciences. [CrossRef]

[4] IEEE SA. (n.d.). *IEEE Standards Association*. IEEE Standards Association. Retrieved from https://standards.ieee.org/ieee/400/7618/

[5] *Finite element analysis for cable rating calculations*. (2025, May 26). Online Library for Electrical Power Systems Publications | eCIGRE. Retrieved from https://www.e-cigre.org/publications/detail/963-finite-element-analysis-for-cable-rating-calculations.html

[6] *IEC 60853-1:1985/Amd2:2008*. (n.d.). IEC WebstoreIEC. Retrieved from https://webstore.iec.ch/en/publication/3708

[7] *IEC TR 62095:2003*. (n.d.). IEC WebstoreIEC. Retrieved from https://webstore.iec.ch/en/publication/6455

[8] *IEC 60287-1-1:2023*. (n.d.). IEC WebstoreIEC. Retrieved from https://webstore.iec.ch/en/publication/68118

[9] IEC 60287-2-1:2023. (n.d.). IEC WebstoreIEC. Retrieved from https://webstore.iec.ch/en/publication/68134

[10] De Leon, F., & Anders, G. J. (2008). Effects of backfilling on cable ampacity analyzed with the finite element method. *IEEE Transactions on Power Delivery, 23*(2), 537-543. [CrossRef]

[11] Dubitsky, S., Greshnyakov, G., & Korovkin, N. (2016, April). Comparison of finite element analysis to IEC-60287 for predicting underground cable ampacity. In *2016 IEEE International Energy Conference (ENERGYCON)* (pp. 1-6). IEEE. [CrossRef]

[12] Wang, P. Y., Ma, H., Liu, G., Han, Z. Z., Guo, D. M., Xu, T., & Kang, L. Y. (2019). Dynamic thermal analysis of high-voltage power cable insulation for cable dynamic thermal rating. *IEEE Access, 7*, 56095-56106. [CrossRef]

[13] Osman, G. F., Elsharkawy, T. M., & Salem, W. A. (2021, December). Thermal analysis of underground distribution cables under dynamic loading in the presence of harmonic load currents. In *2021 22nd International Middle East Power Systems Conference (MEPCON)* (pp. 319-325). IEEE. [CrossRef]

[14] da Silva, M. V., de Araújo, O. M., de Oliveira, D. F., & Lopes, R. T. (2024). Volumetric power density distribution in low voltage cables with Maxwell equations and FEM simulations. *IEEE Transactions on Dielectrics and Electrical Insulation, 31*(4), 2235-2241. [CrossRef]

[15] Greshnyakov, G. V., Egupov, A. A., Dubitsky, S. D., & Korovkin, N. V. (2022, January). Coaxial XPLE-Insulated Cable for Current Pulse Application: Design, Sizing, and Parameters. In *2022 Conference of Russian Young Researchers in Electrical and Electronic Engineering (ElConRus)* (pp. 1180-1184). IEEE. [CrossRef]

[16] Mamaev, K. M., Greshnyakov, G. V., Dubitsky, S. D., Chesnokov, E. A., & Lebedeva, A. A. (2023, November). Transient thermal analysis of coaxial pulse power cable. In *2023 Seminar on Industrial Electronic Devices and Systems (IEDS)* (pp. 167-171). IEEE. [CrossRef]

[17] Morgan, V. T. (2002). The thermal conductivity of crosslinked polyethylene insulation in aerial bundled cables. *IEEE Transactions on Electrical Insulation, 26*(6), 1153-1158. [CrossRef]

[18] Lee, K. Y., Yang, J. S., Choi, Y. S., & Park, D. H. (2006, June). Specific heat and thermal conductivity measurement of XLPE insulator and semiconducting materials. In *2006 IEEE 8th International Conference on Properties & Applications of Dielectric Materials* (pp. 805-809). IEEE. [CrossRef]

[19] Liu, Y., Sun, J., Chen, S., Sha, J., & Yang, J. (2022). Thermophysical properties of cross-linked polyethylene during thermal aging. *Thermochimica Acta, 713*, 179231. [CrossRef]

[20] IEC 60949:1988. (2028, June 30). IEC WebstoreIEC. Retrieved from https://webstore.iec.ch/en/publication/4016

Evgenii A. Chesnokov was born in Russia, in 1998 and received the B.Sc. in electrical engineering from the Perm National Research Polytechnic University and M.Sc. degrees in electrical engineering from the Peter the Great Saint-Petersburg Polytechnic University, Saint Petersburg, Russia in 2020 and 2022, respectively . His current research interests include electrical and high-voltage engineering; electrical insulation, computer simulation, power cables, cable joints, cable terminals, dielectric/conductive polymer-based composites. He is currently an Associate Professor with the Higher School of High-Voltage Engineering, Peter the Great St. Petersburg Polytechnic University. (Email: e-chesnokov@mail.ru)

Efrem G. Feklistov was born in Russia, in 1994 and received the B.Sc. and M.Sc. degrees in electrical engineering and PhD. degree in engineering from the Peter the Great Saint-Petersburg Polytechnic University, Saint Petersburg, Russia, in 2016 , 2018 and 2023, respectively. His current research interests include electrical and high-voltage engineering; electrical insulation, computer simulation, FEM simulation, rotating electrical machines insulation, electrical stress control, corona protection materials, dielectric/conductive polymer-based composites, corona discharge. He is currently an Associate Professor with the Higher School of High-Voltage Engineering, Peter the Great St. Petersburg Polytechnic University. (Email: efrem.feklistov@mail.ru)

George V. Greshnyakov was born in USSR, in 1960 and received the engineer degrees in electrical engineering and PhD. degree in engineering from the Peter the Great Saint-Petersburg Polytechnic University, Saint Petersburg, Russia, in 1983, 1993 respectively,. Received the Dr.Sci from JSC "All-Russian Scientific Research and Development Cable Institute", Moscow, Russia, in 2018. His current research interests include electrical and high-voltage engineering; electrical insulation, computer simulation, power cables, cable joints, cable terminals, dielectric/conductive polymer-based composites. Currently, he is professor of Peter the Great St. Petersburg Polytechnic University, St.-Petersburg, Russia. (Email: g.greshnyakov@gmail.com)

Oleg Emelyanov was born in USSR, in 1961 and received the Dipl.Ing. degree in technical physics and the Ph.D. degree and Dr.Sci. from Peter the Great St. Petersburg Polytechnic University, in 1984, 2004 and 2018, respectively. He has authored over 100 papers in scientific journals and conference proceedings. His current research interests include electrical capacitors, cables, electrical discharges, cold atmospherics and fast exploding wire plasmas. Currently, he is professor of Peter the Great St. Petersburg Polytechnic University, St.-Petersburg, Russia, and Senior Member of IEEE (IEEE DEI and IEEE NPS societies). (Email: oaemel2@gmail.com)